

## Development of Surface Characterisation Toolbox for Additive Manufactured Components: from Planar Layer Surfaces to Complex Functional Surfaces

S. Lou, W. Zeng, L. Pagani, H. Abdul-Rahman, X. Jiang, P. J. Scott

*EPSRC Future Metrology Hub, University of Huddersfield, Queensgate, Huddersfield, HD1 3DH*

[s.lou@hud.ac.uk](mailto:s.lou@hud.ac.uk)

### Abstract

The additive manufacturing (AM) technology possesses the potential to change the paradigm for manufacturing. To facilitate the successful uptake of AM technologies into a wider range of applications, AM needs metrological methods to measure, evaluate, validate techniques for both AM processes and AM parts. Two strategies are proposed for the optimisation of AM processes and the functional evaluation of AM products. A specific procedure is developed for the characterisation of AM layer surfaces with an aim to reflect the unique characterisation of AM process. For complex functional AM surfaces which need the use of X-ray computed tomography (XCT) for their measurement, the surface characterisation techniques are extended so that they can cope with the complex surface shapes and the triangular mesh data.

Additive manufacturing, surface texture, surface characterisation, triangular mesh

### 1. Introduction

Additive manufactured (AM) components are constructed by adding materials layer by layer. Surface topography of the previous layer will affect the following addition, thus the quality of layer surfaces determines that of the whole component. Surface topography is a reflection of AM processes. By looking into these features in a quantitative manner, it can provide valuable feedback information to the optimisation of AM process parameters, e.g. energy density, layer thickness and building orientation [1]. Due to the nature of AM processes, its generated surface topography differs from traditionally manufactured surfaces. Thus the adopted surface characterisation techniques should be able to reflect the unique characters of AM processes.

While examining layer surfaces can provide an insight into the link between AM surface topography and AM process, the measurement and characterisation of the surfaces of complex AM components is also of significant importance for their functional evaluation. However, the difficulty of measuring and analysing these functional AM components lies in their intricate external/internal surface geometries, often freeform shapes, which are intentionally designed for specific functionalities. Conventional tactile and optical measurement methods are not fully eligible to the measurement of these components because of the line-of-sight constraint. XCT is currently the only available non-destructive measurement approach [2-4]. Nonetheless the XCT measurement posts many obstacles to surface texture assessment of AM parts. One of the big issues is that XCT generated measurement data structures, i.e. point cloud and triangular mesh, are not compatible with the standard surface texture characterisation, which requires uniform sampled lattice structure and also requires measured surface to be basically planar.

This paper briefly presents the strategies to overcome these barriers. Firstly, the paper looks into the characterisation of layer surfaces. An updated description of surface wavelength components and topographical features of Powder Bed Fusion

(PBF) surfaces is presented and a procedure to characterise various signature features is developed. Secondly, the general strategy of characterising complex AM surfaces is addressed. Three existing surface filtration (comprising the linear diffusion filter, morphological filters and the 3D watershed segmentation) as well as parameterisation techniques are extended to triangular mesh data structure so that they can be adopted for XCT measurement.

### 2. Updated description of surface wavelength components and topographical features of PBF layer surfaces

AM parts have unusual surface topography that is not comparable to conventionally machined surfaces. This critical fact should be taken into account when characterising AM surface topography, which is often unconsciously neglected. AM processes feature by complex physical interaction that occurs during melting and solidification of materials. Various topographical features are present on AM surface as the signatures of its process. See Figure 1.

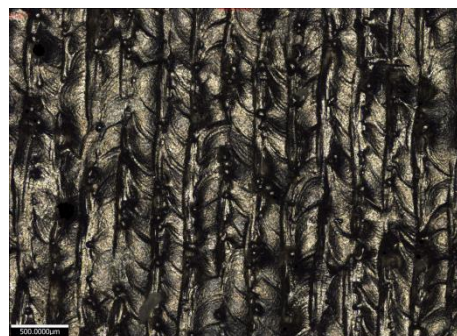


**Figure 1.** Alicon optical image of an Electron Beam Melting (EBM) surface.

- **Roughness:** surface asperity in micro scale. Generated by the physical interaction between the laser beam/electron beam melting process and metal powder particles.
- **Waviness:** wave-like features reflecting the shape of the melted tracks. Formed by the Marangoni flow of molten metal liquid [5].
- **Form error:** Shape distortion. Mainly caused by thermal effect [6].
- **Globules:** spherical protrusion features in various sizes. They can be either small size unmolten/partial molten particles adhered to the underlying surface, or medium size spatters originated from the metal liquid ejection due to molten pool overhear [7], or large size ballings due to insufficient laser energy input or fast laser scanning speed [8].
- **Surface pores:** small cavities in various sizes. Produced by either insufficient power or overhear of the melted pool [9, 10].

### 3. Characterisation of planar AM layer surfaces

#### 3.1. Characterisation strategy

Figure 2 illustrates the proposed procedure to characterise AM processed surfaces. The waviness component is extracted from the measured surface using the advanced filtration techniques. The robust Gaussian regression filter can be a candidate for waviness separation. It incorporates the robust statistical estimation that can provide the filter with the insensitivity against the abnormality, e.g. globules and surface pores. Alternative methods are morphological filters which can achieve similar insensitivity. On the residual surface by excluding the waviness component, the segmentation technique is employed to extract out globules and surface pores, which can be further identified according to their geometry, either convexity or concavity. The roughness component is then taken as the surface portion obtained by excluding the globules and surface pores. It provides the data reference that the roughness parameters will be resulted.

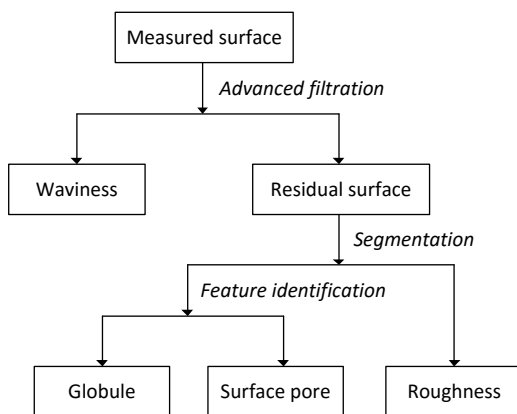


**Figure 2.** Diagram of the proposed surface characterisation procedure for PBF processed surfaces.

#### 3.2. Example

Figure 3(a) presents a 1.42 mm x 1.08 mm surface measured from a top layer surface of a Selective Laser Melting (SLM) component. The robust Gaussian filter is first applied to extract the waviness component. See Figure 3(b). The  $\lambda_c$  cut-off wavelength is intentionally set to 0.08 mm, which is estimated to be the smallest width of the melted tracks. The resulted residual surface, taking off the waviness component from the

original measured surface, comprises the roughness and the globules. See Figure 3(c). The alternative method to separate the waviness is to use the morphological opening filter. Figure 4(a) shows the waviness surface generated by the ball with radius 0.04 mm. Figure 4(b) presents the residual surface.

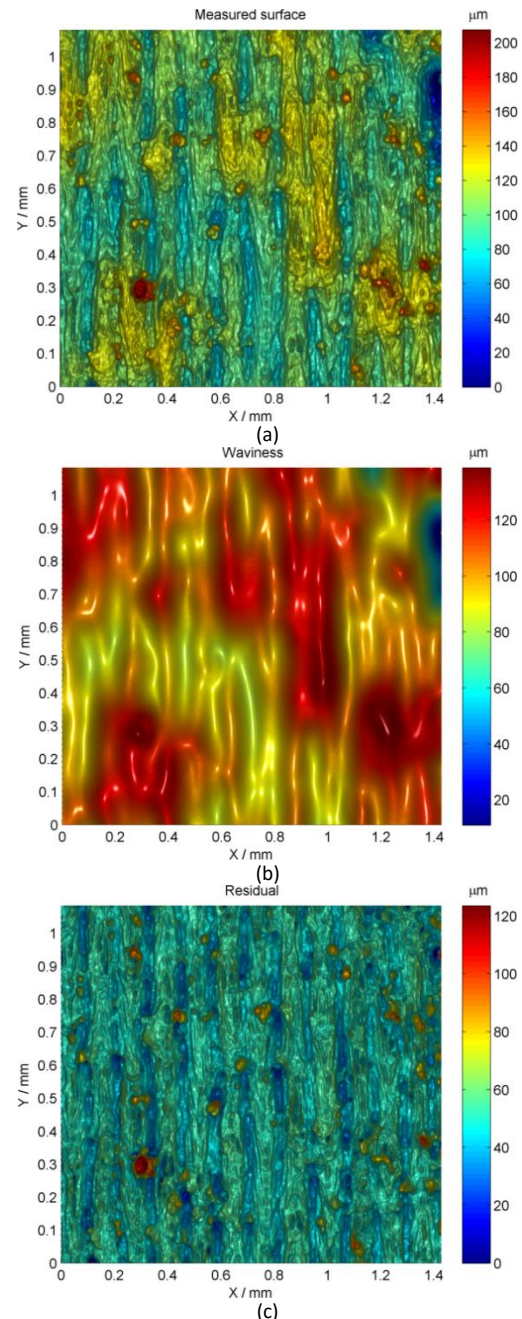


**Figure 3.** Extraction of the waviness of the SLM surface by applying the robust Gaussian filter: (a) measured inclined surface; (b) extracted waviness component; (c) residual surface.

The enhanced watershed segmentation method [11] is then applied to extract the globules out from the residual surface. Take the residual surface generated by the robust Gaussian filter as an example. The developed method is applied to the measured surface with a systematically defined height threshold of 70.5  $\mu\text{m}$ , which is three standard deviations above the mean height of the underlying surface excluding globules. Figure 5(a) illustrates the extracted globules and Figure 5(b) presents the underlying roughness surface.

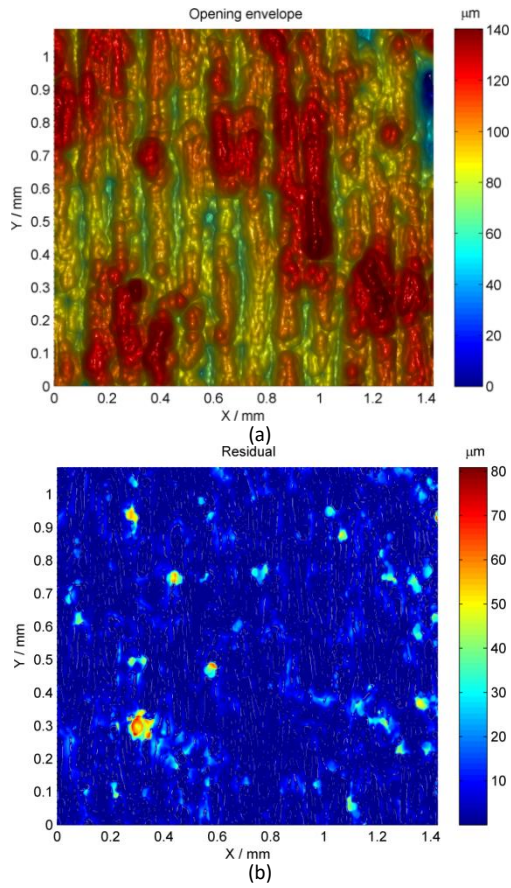


**Figure 4.** Extraction of the waviness of the SLM surface by applying the morphological opening filter: (a) Extracted waviness component; (b) Residual surface.

Table 1 lists four surface texture parameters, i.e.  $S_a$ ,  $S_q$ ,  $S_{sk}$ ,  $S_{ku}$ , for different surface components of the SLM surface, including the waviness surface, the residual surface and the roughness surface (refer to Figure 2). The comparison of these parameters between the residual surface (with the globules on) and the roughness surface (with the globules excluded) reveals the impact of globules on surface texture characterisation. The  $S_a$  and  $S_q$  of the roughness surface is 7% and 24% less than those of the residual surface in that the globules obviously increase the roughness of the surface.  $S_{sk}$  changes from positive value to negative value after excluding the globules, which means the surface changes from a peak dominant case to a valley dominant case. The  $S_{ku}$  value also has a significant change after the exclusion of the globules, which indicates that the globules on the SLM surface have large influence on surface height distribution.

**Table 1** Selected surface texture parameters for different surface components of the SLM surface.

Parameters	Waviness surface	Residual surface	Roughness surface
$S_a$	10.57 $\mu\text{m}$	5.06 $\mu\text{m}$	4.71 $\mu\text{m}$
$S_q$	13.49 $\mu\text{m}$	7.86 $\mu\text{m}$	5.95 $\mu\text{m}$
$S_{sk}$	-	1.30	-0.49
$S_{ku}$	-	12.48	4.72

The parameterisation of globules on the SLM surface is given by Table 2, which consists of the total globule areas, the globule area percentage to the whole surface and the total

globule volume. These parameters are intentionally developed with the aim to offer a meaningful and quantitative evaluation of the globules.

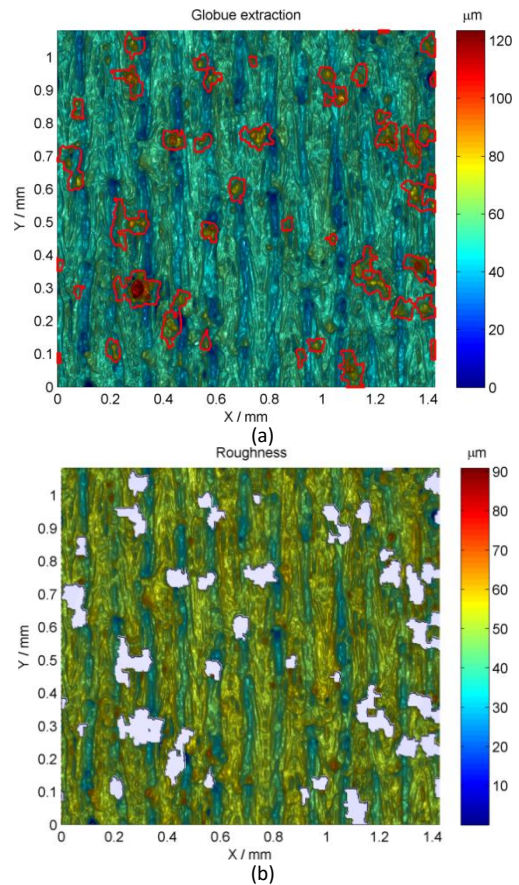


**Figure 5.** Extraction of globules by applying the enhanced watershed segmentation: (a) Boundary of globules; (b) Underlying roughness surface excluding globules.

**Table 2** Parameterisation of the globules of the SLM surface.

Total globule areas	globule area percentage to the whole surface	Total globule volume
0.16 $\text{mm}^2$	10.4%	9.22 $\mu\text{m}^3$

#### 4. Characterisation of complex functional AM surfaces

##### 4.1 General characterisation strategy

Aiming for a holistic assessment of surface texture of complex functional AM surfaces, the adopted strategy is to enhance existing characterisation techniques (including surface filtration and parameterisation) such that they can cope with the complex surface shapes and the triangular mesh data structure as a result of using XCT. In general, the surface texture needs to be extracted such that the desired filtration methods can be applied. The extraction can be achieved through comparing the measured surface with the AM nominal CAD model. The filtration will be based on the residual triangular mesh.

##### 4.2. Filtration techniques

###### (1) Linear diffusion filter

The Gaussian filter is the standard method to separate different wavelength components from surface texture. The prerequisite of applying the Gaussian filter is that the surface under evaluation needs to be planar. The linear diffusion equation can extend the Gaussian filter to freeform geometry [12]. Based on the link between the linear diffusion process and

the Gaussian filtering process, the diffusion time needs to be set to  $t \approx 0.0176\lambda_c^2$ , in order to achieve the same smoothing effect of the Gaussian filter with the cut-off wavelength  $\lambda_c$ .

Figure 6(a) presents an example of applying the linear diffusion filter to a simulated enclosed spherical ball (triangular mesh with 2306 vertices and 4608 faces) [13]. The sinusoidal waves are superimposed to simulate the waviness and the random noises are added as the roughness. The diffusion filter with the diffusion time 1.126 s (equivalent to the Gaussian cutoff wavelength 8 mm) is applied to obtain the reference surface. See Figure 6(b). The roughness component is obtained by comparing the filtered surface to the original surface. The generated height residuals (roughness) are shown as a colour map on the filtered surface. See Figure 6(c).

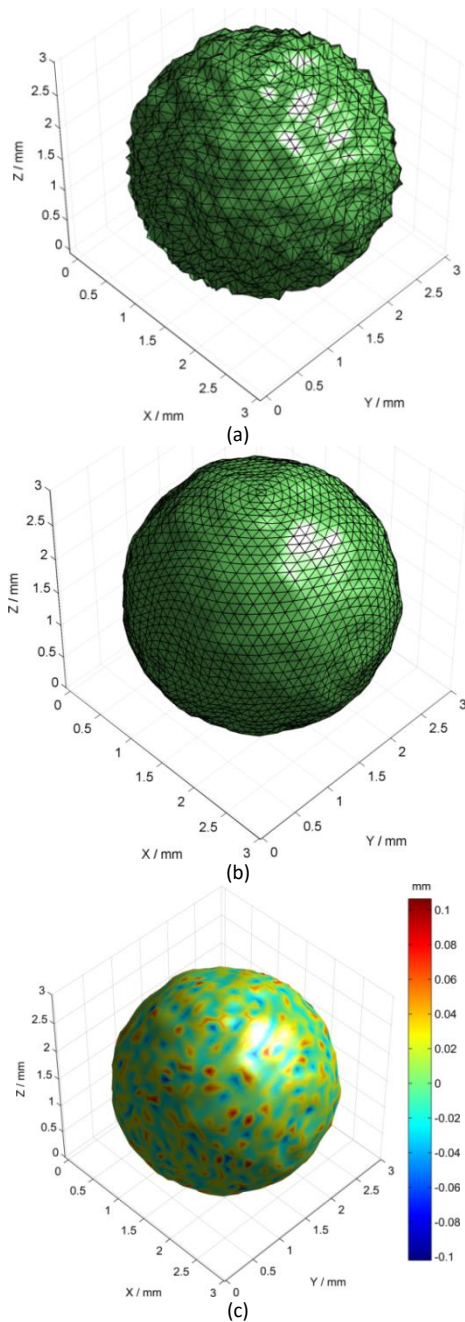


**Figure 6.** The diffusion filtration of a simulated spherical ball: (a) the original simulated surface; (b) the filtered surface; (c) Roughness colour map.

## (2) Morphological filter

Morphological filters emerged as the superset of the early envelope filter. By incorporating the mathematical morphology

theory, it offers more tools and capabilities. The basic variation of morphological filters includes the closing filter and the opening filter, which suppress the valleys and peaks on surface respectively [14] and is more relevant to the functional performance of the product, e.g. tribology [15].

The traditional implementation of morphological operations is based on image processing. While it is efficient for image pixels manipulation, it however cannot be directly applied to surfaces with significant forms. The computational method based on the alpha shape method can be a qualified candidate for morphological filtration of complex AM surfaces [16]. Figure 7 shows the morphological filtration of a saddle shape surface using the alternating symmetrical filter with ball radius 2 mm.

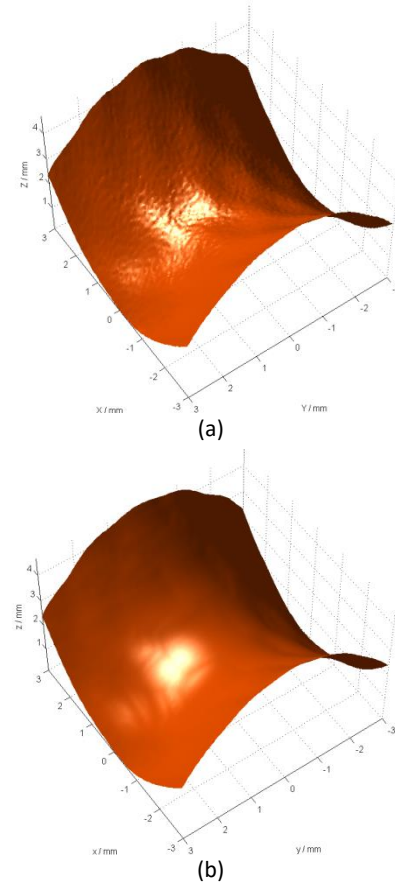


**Figure 7.** Morphological filtration: (a) the saddle surface; (b) the filtered surface.

## (3) Watershed segmentation

The watershed segmentation originated from geography, can naturally segment a landscape into a number of catchment basins (hills or dales). It has been successfully employed to analyse topographical features on engineering surfaces, such as grinding wheels and car body panels [17]. This method can be further extended to the analysis of complex AM surfaces.

Figure 8(a) presents a part of a lattice structure measured using a Nikon XT H 225 industrial CT machine. The reconstructed triangular mesh has a total of 319379 vertices and 634889 faces. A total least squares cylinder has been chosen to estimate form surface. Simulated immersion watershed originally presented in [18] has been used to perform the segmentation. The algorithm uses a scalar field, represented by the scale limited surface, to perform the segmentation of the form surface. The descending watershed segmentation with no Wolf pruning and with 5% Wolf pruning are illustrated in Figure 8(b) and Figure 8(c) respectively. This method can then be used to detect regions with the biggest globules.

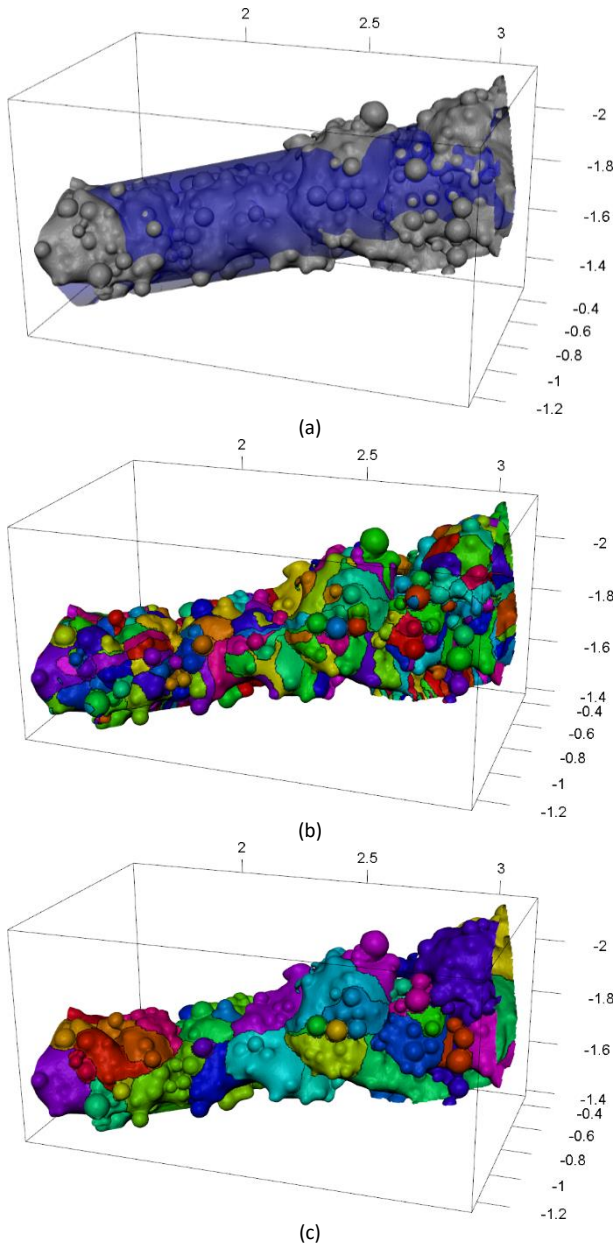


**Figure 8.** 3D Watershed segmentation (values in mm): (a) XCT measured lattice model; (b) Watershed segmentation without Wolf pruning; (c) Watershed segmentation with 5% Wolf pruning.

#### 4.3. Texture parameters' estimation

The extension of areal surface texture parameters defined in ISO 25178-2 is also under development. The triangular mesh version of the commonly used surface texture height parameters are listed in Table 3 along with their discrete implementation for 2.5D surfaces [19].

**Table 3** The extension of height parameters to triangular mesh.

	2.5D	3D
$S_a$	$S_a = \frac{1}{nx \cdot ny} \sum_{i=1}^{nx} \sum_{j=1}^{ny}  z_{i,j} $	$S_a = \frac{1}{A} \sum_{i=1}^{n_{tri}} \sum_{j=1}^6 w_j  z_{ij} $
$S_q$	$S_q = \sqrt{\frac{1}{nx \cdot ny} \sum_{i=1}^{nx} \sum_{j=1}^{ny} z_{i,j}^2}$	$S_q = \sqrt{\frac{1}{A} \sum_{i=1}^{n_{tri}} \sum_{j=1}^6 w_j z_{ij}^2}$
$S_{sk}$	$S_{sk} = \frac{1}{S_q^3 \cdot nx \cdot ny} \sum_{i=1}^{nx} \sum_{j=1}^{ny} z_{i,j}^3$	$S_{sk} = \frac{1}{A \cdot S_q^3} \sum_{i=1}^{n_{tri}} \sum_{j=1}^6 w_j z_{ij}^3$
$S_{ku}$	$S_{ku} = \frac{1}{S_q^4 \cdot nx \cdot ny} \sum_{i=1}^{nx} \sum_{j=1}^{ny} z_{i,j}^4$	$S_{ku} = \frac{1}{A \cdot S_q^4} \sum_{i=1}^{n_{tri}} \sum_{j=1}^6 w_j z_{ij}^4$

More rigorous methods can be referred to [20]. Symmetrical quadrature rules implemented in [21] have been used to perform the integral on a triangular mesh. The parameters estimated with the proposed model correspond to 42.12  $\mu\text{m}$  51.60  $\mu\text{m}$ , -0.86, 2.57 for  $S_a$ ,  $S_q$ ,  $S_{sk}$  and  $S_{ku}$  respectively.

#### 5. Conclusion and future work

The AM technology brings in many advantages that traditional manufacturing technology cannot provide, especially the design freedom. To improve the surface quality of AM processes, the surface characterisation techniques should be used in such a way that the unique characteristics of AM processes can be reflected. Also they will need to be enhanced to meet the requirements of functional evaluation of AM products. Focusing on these two distinct purposes, different strategies are proposed. Specific characterisation techniques are developed or under development for the implementation of these strategies.

The future work will be the full implementation of these characterisation techniques and the application of these techniques for the optimisation of AM processes and the functional evaluation of AM products.

#### Acknowledgement

The authors gratefully acknowledge the UK's Engineering and Physical Sciences Research Council (EPSRC) funding of the Future Advanced Metrology Hub (EP/P006930/1).

#### References

- [1] Taylor J S 2015 *Proceeding of ASPE Spring Topical Meeting – Achieving Precision Tolerances in Additive Manufacturing*, 70-71.
- [2] Kruth, J P, Bartscher, M, Carmignato, S., Schmitt R., De Chiffre L., Weckenmann A. 2011, *CIRP Annals* **60**(2) 821-842.
- [3] Townsend A, Senin N, Blunt L, Leach R K and Taylor J S 2016 *Precis. Eng.* **46** 34–47.
- [4] Thompson A, Maskery I, Leach R K. *Meas. Sci. Technol.* **27** 072001.
- [5] Niu H J, Chang T H 1999 *Scripta Mater.* **41** 1229-1234
- [6] Gibson I, Rosen D W, Stucker B, 2015 *Additive Manufacturing Technologies* (second ed.) Springer
- [7] Simonelli M, Tuck C, Aboulkhair NT, Maskery I, Ashcroft I, Wildman RD, et al. 2015 *Metall. Mater. Trans. A* **46** 3842-3851
- [8] Kruth J P, Froyen L, Van Vaerenbergh J, Mercelis P, Rombouts M, Lauwers B 2004 *J. Mater. Process Technol.* **149** 616-622
- [9] Thijs L, Verhaeghe F, Craeghs T, Humbeek J V, Kruth J -P 2010 *Acta Mater.* **58** (9) 3303–3312
- [10] Tammis-Williams S, Zhao H, Léonard F, Derguti F, Todd I, Prangnell P B 2015 *Mater. Charact.* **102** (4) 47–61
- [11] Lou S, Townsend A, Blunt L, Zeng W, Jiang X 2016, *Proceedings of the 16th EUSPEN International Conference*, University of Nottingham, UK.
- [12] Jiang X, Cooper P, Scott P J 2010 *Proc. R. Soc. A* **467** 841-859.
- [13] Lou S, Abdul-Rahman H, Zeng W, Jiang X, Scott P J 2017 *7th Conference on Industrial Computed Tomography*, Leuven, Belgium.
- [14] Lou S, Jiang X, Scott P J 2014 *J. Phys. Conf. Ser.* **483**: 012020.
- [15] Lou S, Jiang X, Scott P J 2013 *Tribol. T.* **50**(2) 185-193.
- [16] Lou S, Jiang X, Scott P J 2013 *P. Roy. Soc. Lond. A Mat.* **469**(2159): 20130150.
- [17] Scott P J 2004 *Proc. R. Soc. A*, **460** 2845-2864.
- [18] Vincent L and Soille P 1991 *IEEE Transactions on Pattern Analysis and Machine Intelligence*, **13**(6) 583-598.
- [19] Abdul-Rahman H, Lou S, Zeng W, Jiang X., Scott P J 2016, *Measurement* **92** 172-182.
- [20] Pagani L, Qi Q, Jiang X, Scott P 2017 *Measurement* In press.
- [21] Xiao H, Gimbutas Z 2010 *Comput. Math. Appl.*, **59**(2) 663-676.